Supporting Information

Individual Modified Carbon Nanotube Collision for Electrocatalytic Oxidation of Hydrazine in Aqueous Solution

Fato Tano Patrice, Kaipei Qiu*, Li-Jun Zhao, Essy Kouadio Fodjo, Da-Wei Li, and Yi-Tao Long*

Key Laboratory for Advanced Materials, Shanghai Key Laboratory of Functional Materials Chemistry, School of Chemistry and Molecular Engineering, East China University of Science and Technology, 130 Meilong Road, Shanghai 200237, China

*Corresponding author.

E-mail: ytlong@ecust.edu.cn / qiukaipei@ecust.edu.cn. Tel/Fax: 86-21-64252339.

Contents

1. Infrared spectroscopy characterization……...S-3

2. Electrochemical studies…….....S-3

2.1. Electrochemical investigations of MWCNT-NH_2@PQQ modified GCE……...S-3

2.1.1. Effect of the scan rate……...S-3

2.1.2. Kinetic studies through Laviron's method…….S-4

2.2. Electrocatalytic oxidation of N_2H_4 at MWCNT-NH_2 modified GCE and GCE……S-5

2.3. Comparison of electrocatalytic activity for GCE, MWCNT-NH_2, and MWCNT-NH_2@PQQ via voltammetry…….S-6

2.4. Comparison of electrocatalytic activity for GCE, MWCNT-NH_2, and MWCNT-

NH_2@PQQ via chronoamperometry……S-6

3. Single carbon nanotube collision at C UME……S-7

3.1. Collisions between MWCNT-NH_2@PQQ and C UME……S-7

3.2. Collisions between MWCNT-NH_2 and C UME……S-7

4. Single carbon nanotube collisions method to detect H_2O_2……..S-7

5. References……..….S-8

1. Fourier-transform infrared spectroscopy characterization

Fourier-transform infrared (FTIR) spectroscopy, as a powerful technique for studying functional groups attached to the MWCNT surface, was used to ensure that PQQ molecules were integrated on the MWCNT functionalized amino groups. Fig. S1 showed the FTIR spectra of MWCNT-NH_2 (curve a) and MWCNT-NH_2@PQQ (curve b). Both spectra exhibited similar peaks at 3426, 1461 – 1630, and 1051 cm^{-1} corresponding to the amino group (-NH_2), C = C stretching vibration of the MWCNT backbone, and C – N bond stretch vibration, respectively.[1] However, the curve b showed the clear occurrence of some new peaks, such as those at 856 cm^{-1} for the the vibration bond of O – C = O in the carboxylic group, at 1125, 1178, and 1382 cm^{-1} for the C – O bond, and at 3346 cm^{-1} for the –OH stretching vibration.[2] These results clearly supported that the PQQ molecule was successfully attached to the surface of MWCNT-NH_2.

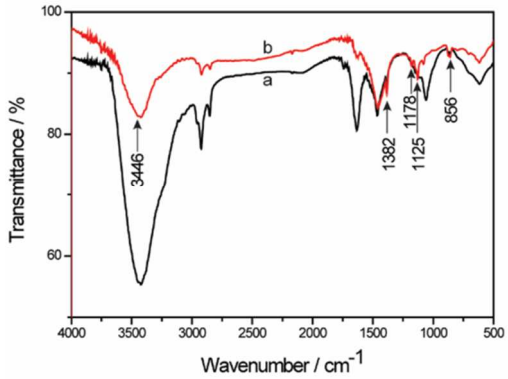

Figure S1: FTIR spectra of a) MWCNT-NH_2 and b) PQQ-modified MWCNT-NH_2 nanocomposites.

2. Electrochemical studies

2.1. Electrochemical investigations of MWCNT-NH_2@PQQ modified GCE

2.1.1. Effect of the scan rate

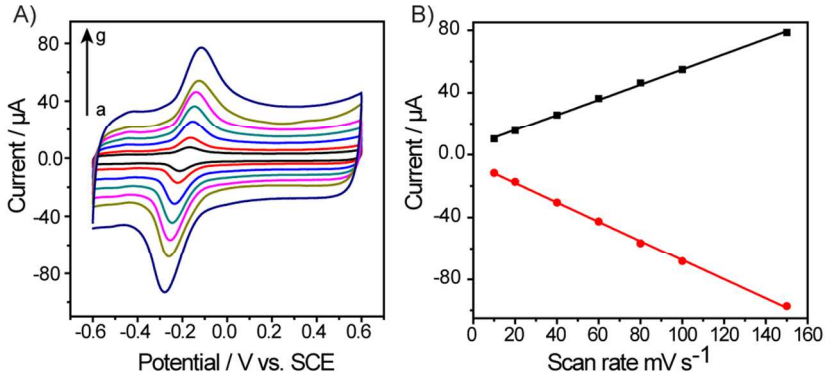

Figure S2. A) CVs of MWCNT-NH_2@PQQ at different scan rates in 0.1 M Tris-HCl buffer (pH 7.0), and B) Relationship between peak currents and scan rates.

2.1.2. Kinetic studies through Laviron's method

Laviron's approach was used to determine the kinetic parameters. The electron transfer rate can be determined by measuring the variation of peak to peak potential separation as a function of scan rate. Thus, Laviron's equation[3] is expressed as follows:

$$E_{P_C} = E^0 + \frac{RT}{\alpha n\mathcal{F}} \ln\left(\frac{RTk_s}{\alpha n\mathcal{F}}\right) - \frac{RT}{\alpha n\mathcal{F}} \ln v \quad (1)$$

$$E_{P_A} = E^0 + \frac{RT}{(1-\alpha) n\mathcal{F}} \ln\left(\frac{RTk_s}{(1-\alpha) n\mathcal{F}}\right) - \frac{RT}{(1-\alpha) n\mathcal{F}} \ln v \quad (2)$$

where E^0 is the formal potential, v represents the scan rate, E_{P_C} and E_{P_A} are the potentials of the cathodic and anodic peaks, respectively, R(8.314 J K^{-1} mol^{-1}) is the universal gas constant, T (K) is the temperature, $\mathcal{F}$ is the Faraday constant , n is the number of electron involved in the reaction process, k_s represents the standard rate constant of the surface reaction, and α is the electron-transfer coefficient .

Figure S3 shows the plots of E_{P_C} and E_{P_A} as a function of $\ln v$ in which the plots of E_{P_C} and E_{P_A} against $\ln v$ were linear. And the equations of the straight line were found to be as follows:

E_{P_A} = -0.7733 + 0.1340 $\ln v$ (R^2= 0.9989) (3)

E_{P_C} = 0.3267 - 0.1206 $\ln v$ (R^2= 0.9992) (4)

E^0 was evaluated to be -0.182 V as the midpoint between the anodic and cathodic peak potentials at low scan rate (10 mV s^{-1}). By using also the slopes of equations (1) and (2) where RT/ $\alpha n\mathcal{F}$ = 0.1340 and RT/ $(1-\alpha)n\mathcal{F}$ = 0.1206, α and n were calculated. And then, ks was also determined using the same plot.

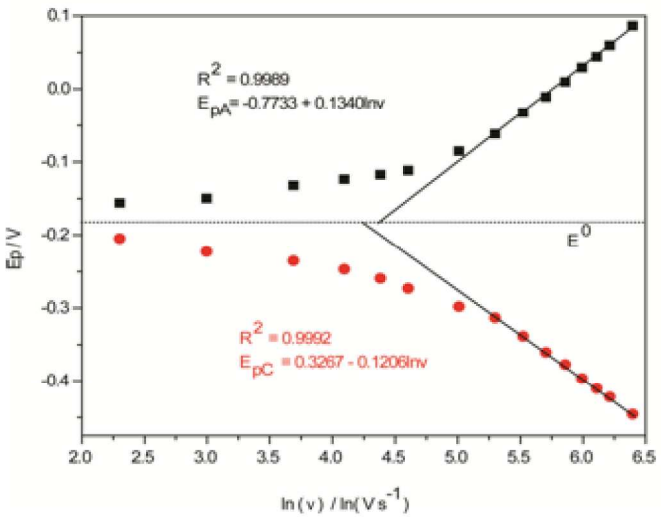

Figure S3. Laviron's plot and the corresponding linear regression for MWCNT-NH_2@PQQ modified GCE in 0.1 M Tris-HCl buffer (pH 7.0).

2.2. Electrocatalytic oxidation of N_2H_4 at MWCNT-NH_2 modified GCE and bare GCE

Figure S4A indicates the CVs from MWCNT-NH_2 modified GCE in 0.1 M Tris-HCl buffer containing different N_2H_4 concentrations (1, 2, 4, 8, and 10 mM). As shown, the

oxidation peak increases with increase in the concentration of N_2H_4. Meanwhile, any reduction peak potential was observed, suggesting that MWCNT-NH_2 has also a catalytical activity toward N_2H_4 oxidation. This result was likely assigned to the electrocatalytic of carbon nanotubes due to the presence of edge-plane-like sites in the CNTs [4]. Figure S4B presents the (i-t) curves of MWCNT-NH_2 modified GCE in 0.1 M Tris-HCl buffer at one potential level, + 0.5 V versus SCE in the presence of N_2H_4 concentration varying from 0 to 10 mM. As seen, the amperometric signal increases with increasing N_2H_4 concentration at 120 s. This result shows a catalytic effect of MWCNT-NH_2 modified GCE to N_2H_4 oxidation which could be ascribed to the electrocatalytic onto CNTs surface.

Figure S4C indicates the CVs from bare GCE after altering the concentration of N_2H_4 ranging from 1 to 10 mM in 0.1 M Tris-HCl buffer (pH 7.0). Despite the slight increase in anodic current, the CV shows no redox peak indicating that the GCE has no catalytical activity toward N_2H_4 oxidation. To further show the no catalytic effect of the bare GCE, it chronoamperometric study was done. Thus, Fig. S4D indicates the chronoamperograms of bare GCE in 0.1 M Tris-HCl buffer at one potential level, + 0.5 V versus SCE in the presence of various concentrations of N_2H_4 (0 – 10 mM). Through this Figure, at zero concentration of N_2H_4, the current is nil. And, when the concentration of N_2H_4 increases the anodic currents were found in "stacking form" illustrating that the bare GCE does not catalyze N_2H_4 oxidation.

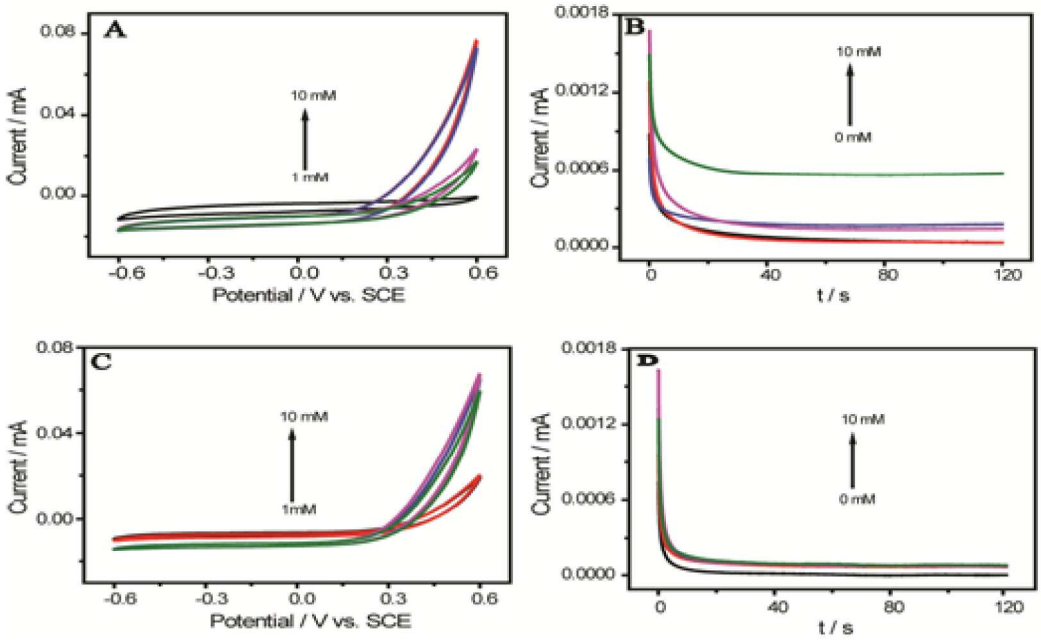

Figure S4. A) CVs from MWCNT-NH_2-modified GCE in 0.1 M Tris-HCl buffer (pH 7.0) in the presence of N_2H_4 at different concentrations (1, 2, 4, 8, and 10 mM) and B) its resulting chronoamperograms at +0.5 V vs. SCE read at 120 s. C) CVs of the bare GCE in 0.1 M Tris-HCl buffer (pH 7.0) in the presence of N_2H_4 at different concentrations (1, 2, 4, 8, and 10 mM) and D) its resulting chronoamperograms at +0.5 V vs. SCE read at 120 s. The black curves in B and D represent the CAs from MWCNT-NH_2-modified GCE and bare GCE in the supporting electrolyte, respectively.

2.3. Comparison of electrocatalytic activity for GCE, MWCNT-NH_2, and MWCNT-

NH_2@PQQ via voltammetry

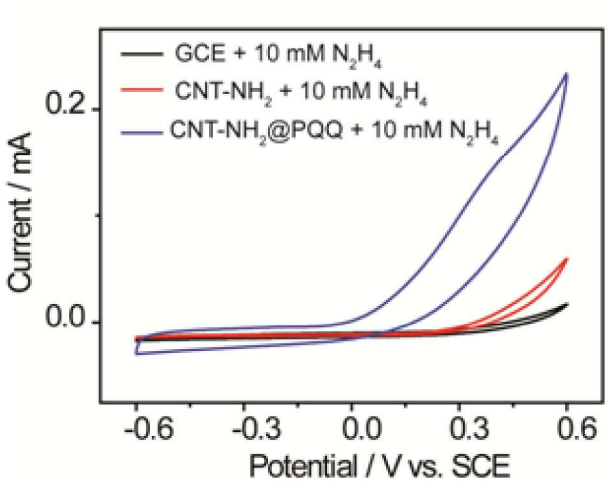

Figure S5. Comparison of CVs from GCE (black curve), CNT-NH_2 (red curve), and CNT-NH_2@PQQ (blue curve) in 0.1 M Tris-HCl buffer (pH 7.0) containing 10 mM N_2H_4. The scan rate was 100 mV s^{-1}.

2.4. Comparison of electrocatalytic activity for GCE, MWCNT-NH_2, and MWCNT-NH_2@PQQ via chronoamperometry

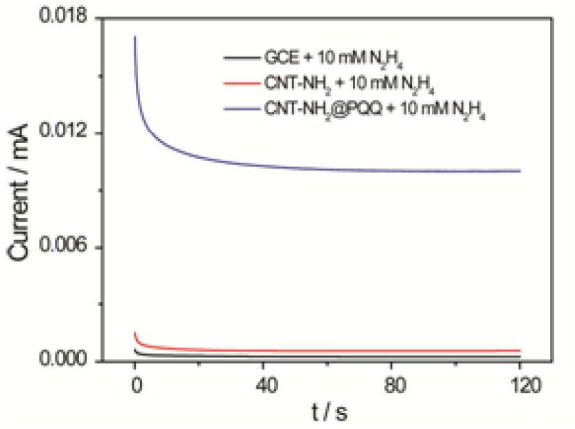

Figure S6. Comparison of CAs obtained from GCE (black curve), CNT-NH_2 (red curve), and MWCNT-NH_2@PQQ (blue curve) in 0.1 M Tris-HCl buffer (pH 7.0) containing 10 mM N_2H_4. The CA was recorded at a potential of +0.5 V vs. SCE and the currents read at 120 s.

3. Single carbon nanotube collision at C UME

3.1. Collisions between MWCNT-NH_2@PQQ and C UME

Figure S7. Impacting events from 2 mg/mL MWCNT-NH_2@PQQ colliding with C UME at 1.0 V in Tris-HCl (0.1 M, pH 7.0) without the addition of 10 mM N_2H_4.

3.2. Collisions between MWCNT-NH_2 and C UME

Figure S8. Chronoamperometric data for collisions between 2 mg/mL MWCNT-NH_2 and C UMEs in 0.1 M tris-HCl buffer (pH 7.0) at 1.0 V in the a) absence and b) presence of 10 mM N_2H_4.

4. Single nanoparticle collision method to detect H_2O_2

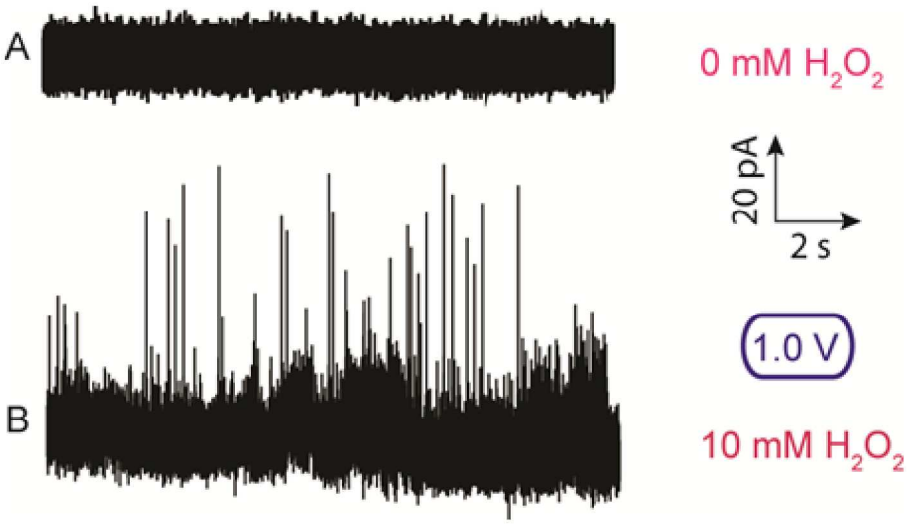

Figure S9. Chronoamperometric data for collisions between 2 mg/mL MWCNT-NH_2 and C UMEs in 0.1 M tris-HCl buffer (pH 7.0) at 1.0 V in the a) absence and b) presence of 10 mM H_2O_2.

4. References

(1) Al-Shuja'a, O.; Obeid, A.; El-Shekeil, Y.; Hashim, M.; Al-Washali, Z. New Strategy for Chemically Attachment of Imine Group on Multi-Walled Carbon Nanotubes Surfaces: Synthesis, Characterization and Study of DC Electrical Conductivity. *J. Mater. Sci. Chem. Eng.* **2017**, *5* (2), 11–21.

(2) Al-Shuja'a, O.; Obeid, A. O.; Al-Shekeil, Y. A.; Salit, M. S.; Al-Washali, Z. A. Synthesis, Characterization and Study of DC Electrical Conductivity of Poly[MWCNT/Ester] Composites. *TuJnaS*, **2016**, *A* (6), 105–119.

(3) Ma, W.; Li, D. W.; Sutherland, T. C.; Li, Y.; Long, Y. T.; Chen, H. Y. Reversible Redox of NADH and NAD + at a Hybrid Lipid Bilayer Membrane Using Ubiquinone. *J. Am. Chem. Soc.* **2011**, *133* (32), 12366–12369.

(4) Cardoso, R. M.; Montes, R. H. O.; Lima, A. P.; Dornellas, R. M.; Nossol, E.; Richter, E. M.; Munoz, R. A. A. Multi-Walled Carbon Nanotubes: Size-Dependent Electrochemistry of Phenolic Compounds. *Electrochim. Acta* **2015**, *176*, 36–43.